

**In-flight icing hazard detection
with dual and single-polarimetric moments from operational NEXRADs**

David J. Serke*^a, Scott Ellis^b, John Hubbert^b, David Albo^a,
Christopher Johnston^a, Charlie Coy^a, Dan Adriaanson^a and Marcia K. Politovich^a

^a NCAR- National Center for Atmospheric Research
Research Applications Laboratory
Boulder, Colorado

^b NCAR- National Center for Atmospheric Research
Earth Observing Laboratory
Boulder, Colorado

1. INTRODUCTION

Liquid water with a temperature below the 0°C freezing value is termed 'supercooled liquid water' (SLW) and can be a danger to aircraft. SLW that comes in contact with an aircraft's superstructure freezes onto it and negatively impacts aerodynamic characteristics. The aviation community therefore has an interest in the capability to detect and warn on in-flight icing hazards.

No single instrument has yet been developed which can remotely and unambiguously detect in-flight icing conditions within a volume of airspace. For this reason, combinations of sensors and/or numerical weather prediction (NWP) models have been under development for some time to detect in-flight icing (Politovich et al, 1995, Bernstein et al., 2005). NASA's Icing Remote Sensing System (NIRSS) is a prototype used to detect in-flight icing using passive radiometry and a K_a-band radar that has been under development by NASA and NCAR since 2003 (Reehorst et al., 2006). Ka-band radars have shorter wavelengths than S-band precipitation radars such as NEXRADs and have been shown to be more sensitive to cloud and small-drop (> 50 μm diameter) icing. Since the power returned to the radar receiver is proportional to the sixth power of the particle

diameter, larger particles such as ice crystals and conglomerates tend to dominate over the typically smaller liquid drops, which are of interest in in-flight icing. For this reason, in-flight icing detection with single-polarization S-band weather radars has historically not been feasible.

Single-polarization S-band weather radars transmit and receive only a single horizontal polarization of radiation, and only measure reflectivity (REFL), radial velocity and spectrum width. The National Weather Service has recently completed the process of upgrading the national network of NEXRADs in the lower forty-eight states with the capability of transmitting and receiving both vertically and horizontally oriented waves – known as 'dual-polarization'. Dual-polarized radars collect additional information that can provide insight as to the mean particle shape, size, phase (liquid or solid), bulk density and preferred particle orientation in a given sample volume. Polarized radars can collect moment fields such as differential reflectivity (Z_{dr}), correlation coefficient (ρ_{HV}), linear depolarization ratio (LDR) and specific differential phase (KDP) as well as the previously mentioned single-polarization moments (Bringi and Chandrasekar, 2001). Dual-polarization moment characteristics that are relevant to in-flight icing are discussed in Section 2.

In 2009, NCAR began subcontracting with MIT Lincoln Labs and the FAA (Smalley et al., 2009) to develop a prototype Icing Hazard (IH) algorithm for detecting in-flight icing with dual-polarization S-band radars. This initial study utilized one case from the Australian CP2

*Corresponding author address: David J. Serke,
National Center for Atmospheric Research, PO
Box 3000, Boulder, CO 80307,
dserke@ucar.edu

research radar and one case from the Colorado State University CHILL research radar along the Front Range of Colorado, both of which have similar characteristics to polarized NEXRADs. These radars were used since few polarized operational radars were available at the time. Early findings (Ellis et al., 2011) showed that the IH output was physically consistent with the presence of supercooled liquid water (SLW) aloft. A follow-on project in 2011-2012, sponsored again by MIT and the FAA, led to further testing and tuning of the algorithm. For this study period, NIRSS was positioned between CSU-CHILL and Denver International Airport so that Pilot Reports (PIREPs) of icing could be reasonably represented by the ground-based sensing platforms. Findings from this field campaign (Serke et al., 2011, Albo et al., 2012) found that the algorithm generally detected icing in the vicinity of icing PIREPs, but could miss small-drop cases that were below the minimum detectable signal-to-noise ratio. In 2012-2013, NCAR began work on an FAA funded project using the National Weather Service's network of operational S-band NEXRADs. An initial study using limited operational polarized NEXRAD cases (Serke et al., 2012) found that radar volumes that contained moderate or greater severity icing PIREPs had significantly larger percentage of pixels identified as 'yes icing' by IH. The inverse was found to be true for null PIREPs as related to 'no icing' output.

The main goal of this study is to determine if there is a quantifiable benefit to dual-polarization over single-polarization moments in a radar-based in-flight icing detection algorithm. In this work, the polarized algorithm is stripped of all polarized moment input and then parallel single-polarization versions are processed and analyzed for 75 total moderate or greater (MOG) and Null in-flight icing severity cases from 2012 to early 2013. The second goal of this field campaign was to test and improve the prototype NIRSS. Results are compared to NIRSS output over Cleveland when possible.

Section 2 describes the in-flight icing input data sources and algorithms. A definition of the statistical representation leading to probabilities of each algorithm detecting MOG or Null icing severity PIREPs is presented in Section 3. Two sample case studies are highlighted in Section 3,

and the statistical results of the 75 cases studies are discussed in Section 4. The findings on the benefits of dual-polarization moments to radar-based detection of in-flight icing are in Section 5, and the paper is summarized in Section 6.

2. Icing Data and Algorithms

2.1 Radar 'Icing Hazard'

Differential reflectivity is the ratio of horizontal co-polar received power to the vertical co-polar return. One way to interpret this field is a power-weighted mean axis ratio of the particles in the volume. Small liquid and cloud drops are nearly round, so Zdr values are near zero and have low reflectivity. Larger drops become oblate as they fall with Zdr between 0.3 and 2.0 dB. Oriented ice crystals also have Zdrs that are positive and large. ρ_{HV} is the correlation between horizontal and vertical co-polar received returns. Wet or tumbling particles and mixed phase conditions result in decorrelation in polarizations so that ρ_{HV} values are typically below 0.92. Homogeneous rain or ice result in ρ_{HV} values above 0.95. KDP, or specific differential phase, is the range derivative of the differential phase shift between the horizontal and vertical pulse phases in degrees per kilometer. KDP values near zero tell us that nearly round particles dominate in a given radial. Care must be given to areas of low signal-to-noise ratio as KDP becomes very noisy.

The polarized radar-based icing hazard algorithm (Figure 1) detects the melting level using reflectivity, Zdr and ρ_{HV} (Albo et al., 2012) and adjusts an inputted NWP model-based temperature sounding accordingly. A dual-polarization algorithm for particle identification is used next in order to filter out particle types that IH is not interested in, such as warm rain, clutter and biological targets. Two meta-algorithms that utilize fuzzy logic-based membership functions are then implemented for detecting freezing drizzle and mixed-phase conditions along each radar tilt. The mixed-phase algorithm utilized spatial tendencies in KDP and Zdr (Plummer et al., 2010) and the freezing drizzle algorithm uses spatial textures of reflectivity (Ikeda et al., 2009) to infer in-flight icing situations. The IH algorithm uses thresholds on

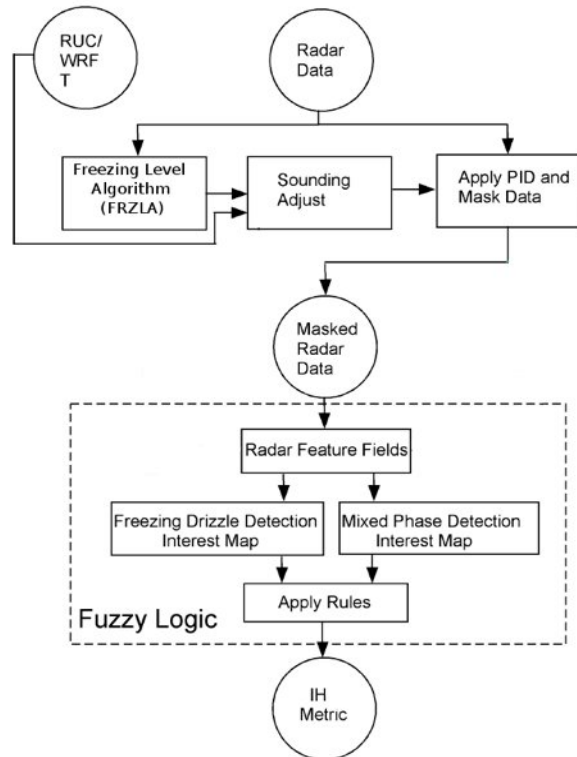


Figure 1. Radar 'Icing Hazard' Algorithm flow diagram.

the outputted interest fields from the individual meta-algorithms to define 'yes', 'maybe' or 'no icing' at each pixel within the radar volume.

To prove the utility of dual-polarization in NEXRAD radar-based in-flight icing detection, a parallel IH algorithm was created where all dual-polarization components were stripped from the process. These changes involve removing the Zdr and ρ_{HV} components of the melting level detection algorithm, the entire particle identification algorithm, the entire SLW detection algorithm and then adjusting the final IH icing classification rules to account for the missing polarization components. So as not to completely discount the usefulness of single-polarization NEXRAD, a third version of IH was created that added back a new SLW fuzzy logic module based on the relative frequency of occurrence of SLW during in-situ research flight campaigns compared to reflectivity (Hudak et al., 2002) and temperature (Cober et al., 2001). These three algorithms are abbreviated for the rest of this work as follows:

- IHL_{DP} = Dual-polarization version (Figure 1)
- IHL_{SP-y} = Single-polarization version with a new SLW module that utilizes ILW relations to reflectivity and temperature
- IHL_{SP-n} = Single-polarization version with no SLW module at all

2.2 NIRSS

NIRSS consists of a vertically pointing Doppler K_a-band radar, a multichannel radiometer and a laser ceilometer (Reehorst et al., 2006). The Model 3000 multi-channel radiometer by Radiometrics Corporation passively collects incoming microwave radiation at a number of channels in the K_a and V-bands of the electromagnetic spectrum (Solheim et al., 1998). The K_a-band lies within an atmospheric window and thus variations at specific frequencies within the band are due to variations in the amount of liquid and gaseous water. Different amounts of gaseous and liquid phase water cause the amount of microwave radiation received by the radiometer at frequencies within the K_a-band to respond differently. Algorithms used within the radiometer's software compare the integrated liquid water (ILW) and integrated water vapor (I WV) of large historical archives of station sounding data to the inverted radiometric brightness temperatures from the instrument in order to arrive at ILW and IWV values for a given real-time radiometer profile. The V-band is on the shoulder of a major oxygen absorption feature, so that progressively varying frequencies from the peak of the absorption feature yields information on the atmospheric temperature further from the radiometer in range. This allows for the derivation of an atmospheric temperature profile. Input data streams are ingested into a fusion machine which is used to combine the instrument fields into an in-flight icing product. The height range of the 0 and -20° Celsius isotherms are targeted as the region where in-flight icing could exist. The vertical extent of cloud boundaries are provided by the ceilometer and K_a-band cloud radar. The ILW is distributed regardless of the temperature range, although temperature at cloud top helps determine how it is distributed. ILW is distributed vertically with fuzzy logic based on previous experience with years of research flights in icing conditions (Reehorst et al., 2005). The mandate of the NIRSS

program is to detect in-flight icing in the near-airport environment with existing, relatively inexpensive technologies. A recent study found that NIRSS detects the absence, presence and severity of in-flight icing at least as well as the FAA's current operational system to detect icing (Johnston et al., 2011).

2.3 Pilot Reports

Pilot Reports (PIREPs) are voluntary reports made by pilots of the time and location of significant meteorological conditions encountered during flight. In-flight icing is one of many possible conditions that can be reported. The existence of icing can be reported as 'no icing exists' (or 'null icing') or 'icing exists' as 'trace', 'light', 'moderate', 'severe' or 'heavy' severity. For this study, the top three categories of icing severity are lumped together as one 'moderate or greater' ('MOG'). Only PIREPs within 100 km of a dual-polarized NEXRAD are considered.

2.4 'Precipitation Identification Near the Ground' (PING)

PING is a project to collect weather information from the public through their mobile device. The free online application records time, location and precipitation type and data are stored to a database. The link address used to provide case precipitation type is: <http://www.nssl.noaa.gov/projects/ping>.

3. Method

In order to characterize whether an icing detection algorithm successfully matches a given PIREP's icing severity and location, a quadrant is defined within the radar volume that matches the PIREP closest in time. A PIREP's location relative to the corresponding NEXRAD is plotted and matched to the a radar volume centered on a 90 degree azimuth quadrant. If 10% or more of the radar return in the designated quadrant is warned on as 'yes icing' by a given icing detection algorithm, it is considered a match to that PIREP within that quadrant. A value of 10% of a quadrant's pixels is chosen because previous research flights have shown that significant SLW

can exist in pockets and needn't cover the entire volume to have significant effects on an aircraft's flight. The probability of detecting a 'yes icing' PIREP (POD_y) for each algorithm is the fraction of cases that each algorithm properly detects as a 'yes icing' case in relation to the MOG PIREP icing severity, divided by the total number of 'MOG' PIREPs under consideration. Conversely, if 90% or more of the radar return within this quadrant is warned as 'no icing' or 'maybe icing', it is considered a match to a Null PIREP. The probability of detecting a Null PIREP (POD_n) for each algorithm is the fraction of cases that each algorithm detects as a 'no icing' or 'maybe icing' cases divided by the total number of Null cases. No attempt is made to quantify the IH icing algorithms' detection efficiency with height as the quadrant volumetric method described above was deemed sufficient.

NIRSS is considered a match to a MOG PIREP's icing severity designation if MOG severity appears anywhere in the profile within 10 minutes of the PIREP time. The same time constraint is true of NIRSS for Null PIREPs if NIRSS records 'trace' or less icing severities.

4. Case Studies

For this study, 50 MOG and 25 Null icing PIREPs were selected and compared to output from the four ground-based remote sensing algorithms which detect in-flight icing hazards, as described in Sections 2.1 and 2.2. Case selection was an effort to balance the desire to represent all known categories of atmospheric conditions that lead to in-flight icing, with the secondary goals of having NIRSS available for comparison and achieving geographical diversity.

Typical output for the three IH algorithm versions introduced in Section 2.1 are shown for a sample MOG (Figure 2) and Null PIREP (Figure3). In each figure subplot a is reflectivity, b is IH_{DP} , c is IH_{SP-y} and d is IH_{SP-n} . The polarized NEXRAD is at the center of the plot (coordinates 0,0) and the units are in kilometers. PIREP location is shown with a pink '+' symbol, and the quadrant where IH output was considered a match to the PIREP is shown as a black polygon. The scale for the three IH outputs correspond to blue

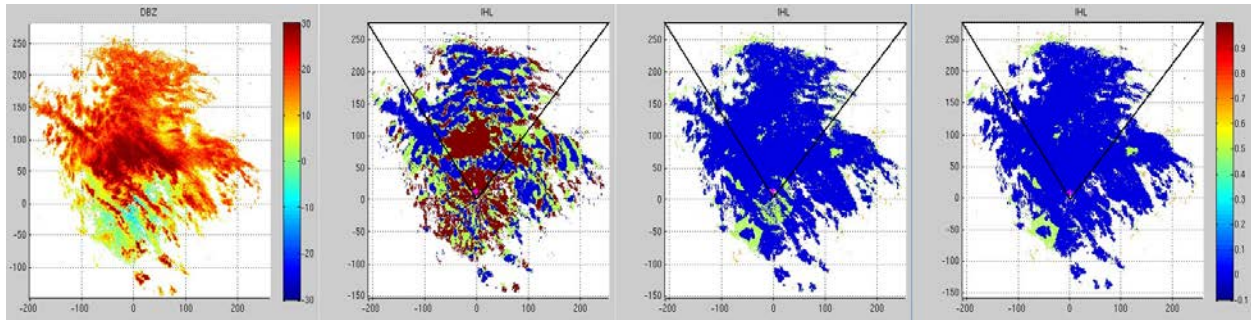


Figure 2. Reflectivity (a), IH_{DP} (b), IH_{SP-y} (c) and IH_{SP-n} (d) for a MOG PIREP case from February 22nd, 2013 at KCLE.

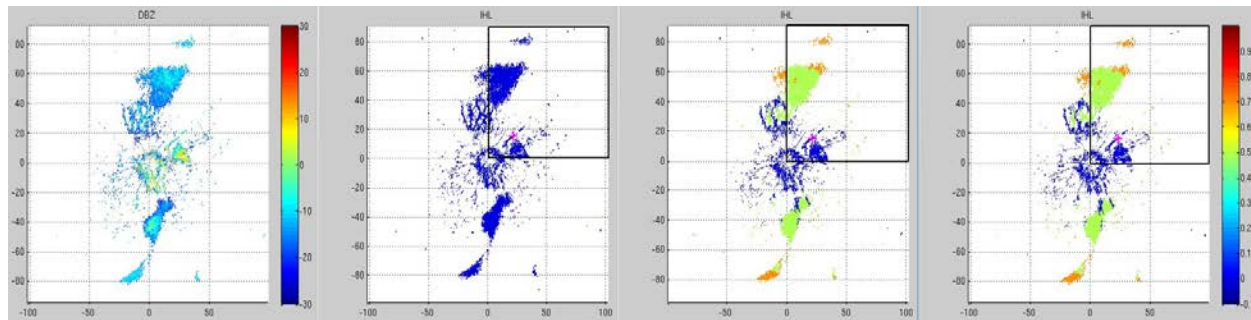


Figure 3. Reflectivity (a), IH_{DP} (b), IH_{SP-y} (c) and IH_{SP-n} (d) for a null PIREP case from February 22nd, 2013 at KCLE.

as 'no icing', green as 'maybe icing', orange as 'icing yes due to freezing drizzle' and red as 'icing yes due to mixed phase SLW'. A publicly accessible web page with plots and discussion for each of the 75 cases is available for viewing at the following address: <https://wiki.ucar.edu/display/icinghazardlevel/Home>.

5. Results

The resulting statistics for the 75 MOG and Null categories are shown in Table 1. Categories for atmospheric SLW production mechanism (left column) are loosely based on work done by Bernstein et al., (1997), which related aircraft icing to synoptic-scale weather conditions. The center block of columns shows total PIREPs for each mechanism and the corresponding number of cases matched correctly by each IH algorithm, followed by a summation row. POD_y and POD_n are calculated on these summed case numbers. The right hand block of

Table 1. Number of MOG (top) and Null (bottom) PIREPs and matches to PIREP icing classification for four icing algorithms with resulting POD_y and POD_n .

Weather Scenario	# of MOG matched by algorithm...			
	PIREPs	IH_{SP-n}	IH_{SP-y}	IH_{DP}
Dev. low/upslope	25	2	7	21
shortwave trough	3	0	1	3
stationary front	0	0	0	0
ahead warm front	5	3	3	5
behind cold front	8	2	5	8
lake effect	8	0	4	7
hurricane/ext. Trop.	1	0	0	1
TOTAL CASES	50	7	20	45
POD_y		0.14	0.40	0.90

Weather Scenario	# of Null matched by algorithm...			
	PIREPs	IH_{SP-n}	IH_{SP-y}	IH_{DP}
TOTAL CASES	25	22	13	15
POD_n		0.88	0.52	0.60

columns is the same but for NIRSS cases at Cleveland, Ohio. The PING network was utilized to provide surface precipitation type for each case.

A wide range of SLW production mechanisms were sampled with the 50 MOG cases. In most cases, 10 to 60% of the pixels within the quadrant were warned on as 'yes icing' by $I_{H_{DP}}$. Most of the time, the positive icing regions were cellular in nature and the majority of the pixels within the PIREP quadrant were not positive for icing. Positive $I_{H_{DP}}$ for all SLW mechanisms tended not to exist in areas of maximum reflectivity, rather in areas of relative minimum reflectivity. Cases that were dynamically developing tended to have most positive icing area from the mixed phase algorithm (dark red). Longer-lived cases tended to have a fringe of positive icing at cloud top due to the freezing drizzle algorithm (orange) plus mixed phase areas within the reflectivity column. Several cases had no mixed phase pixels with positive icing and instead had only large percentages of pixels as positive icing from the freezing drizzle algorithm. For the 40% of MOG cases correctly identified by the $I_{H_{SP-y}}$ algorithm, a continuous ring of pixels tended to be highlighted as positive icing as opposed to cellular features in $I_{H_{DP}}$. $I_{H_{DP}}$ also tended to detect icing at lower levels than $I_{H_{SP-y}}$, probably due to the increased freezing layer height precision afforded by the Zdr and ρ_{HV} dual-polarization moments.

Five of the 'developing low/up-slope' cases correspond to observations of graupel at the surface, a marker for SLW aloft, as the micro-physical production of this species is dependent on riming by SLW. These graupel cases and others yet to be processed will be targeted for closer examination in the future, as Zdr values in previous studies (Evaristo et al., 2013) have been found to be slightly negative. Perhaps a new module specific to graupel detection could be explored.

All five of the MOG cases in the 'ahead of warm front' category corresponded to freezing rain at the surface. $I_{H_{SP-n}}$ performed better than in other forcing categories as it relies on the reflectivity texture-based freezing drizzle algorithm. Findings from these cases suggest that the single-polarization freezing drizzle product is working reasonably well.

In lake effect-induced icing cases, $I_{H_{SP-n}}$ tended to reverse SLW location within precipitation bands and call out 'icing=no', when compared to $I_{H_{DP}}$.

Overall, NIRSS and $I_{LW_{DP}}$ had similarly high icing detection capability. The relation between these two radically different icing detection algorithms is highly dependent on the respective definitions of detection and non-detection between the vertically pointing NIRSS and the volumetric NEXRAD radar algorithms. These simplistic definitions, discussed in Section 3, do however elucidate the large differences in detection afforded by utilizing dual polarization. Overall, $I_{H_{SP-n}}$ had a relatively poor MOG icing detection rate of 0.14. The $I_{H_{SP-y}}$ addition had a significant improvement over $I_{H_{SP-n}}$ (0.40 versus 0.14), but the addition based on reflectivity and temperature still had less than half of $I_{H_{DP}}$ detection rate of 0.90. $I_{H_{SP-n}}$ had a high detection rate of Null icing since it had a poor overall capability of detecting icing without polarization (i.e. Most of the radar echo was categorized as 'no icing'). $I_{H_{DP}}$ and $I_{H_{SP-y}}$ generally detected over half of Null cases correctly. NIRSS had the best detection rate for Null icing (0.72), which was a similar finding to previous work (0.71 in Johnston et al., 2011).

6. Summary

In-flight icing can be a significant hazard to aircraft and detecting and warning on its existence is a priority for the FAA. NCAR has been working since 2009 on an algorithm using polarized S-band NEXRAD weather radars, as well as continuing development with NASA of NIRSS. In this study, it was found that where there was detectable S-band signal above the noise threshold, operational NEXRADs had a very high icing detection rate over a wide variety of forcing mechanisms and surface precipitation types compared to icing PIREPs. There still remains a whole category of icing cases that may not be detectable by S-band weather radars, whose relative frequency should be determined in future studies. The National Severe Storms Laboratory, in collaboration with NCAR, is testing a new noise filter based on ρ_{HV} which aims to retain more of the low signal reflectivity areas. This product could significantly boost the IH ability to detect small-

drop cases, at least in airport terminal areas within 15 km of the radar. Modules to detect high Zdr bands within precipitation and to detect negative Zdr in graupel will be tested and implemented in the upcoming year. There is also the possibility of a research flight campaign in 2014-2015 in the Great Lakes Region to further test the ground based remote sensing algorithms discussed within. Geographic diversity of icing across the US should also be pursued further.

Acknowledgments

This research is in response to requirements and funding by the Federal Aviation Administration (FAA). The views expressed are those of the authors and do not necessarily represent the official policy or position of the FAA.

References

- Albo, D., Ellis, S., Serke, D., Weekley, A., Adriaansen, D., Johnston, C., Politovich, M., Dixon, M. and Hubbert, J., "Icing Hazard Level: Final Report 2011-2012", *Deliverable to MIT Lincoln Laboratory*, 64 pp., 2012.
- Bernstein, B.C., T.A. Omeron, F. McDonough and M.K. Politovich, "The relationship between aircraft icing and synoptic scale weather conditions", *Wea. Forecasting*, **12**, 742-762, 1997.
- Bernstein, B., McDonough, F., Politovich, M., Brown, B., Ratvasky, T., Miller, D., Wolff, C., and Cunning, G., "Current Icing Potential: algorithm description and comparison to aircraft observations", *J. Appl. Meteor.*, **44**, pp. 969-986, 2005.
- Bringi, V. and Chandrasekar, V., "Polarimetric Doppler Weather Radar – Principles and applications.", *Cambridge University Press*, 656 pp., 2001.
- Cober, S., Isaac, G., Korolev, A. and Strapp, W., "Assessing cloud-phase conditions", *J. of Appl. Meteor.*, **40**, pp. 1967-1983, 2001.
- Ellis, S.M., D.Serke, J. Hubbert, D. Albo, A. Weekley and M.K. Politovich, "In-flight icing detection using S-band dual-polarimetric weather radar data". *AMS 35th Conf. on Radar Meteor.*, Pittsburgh, PA, 26-30 September, 2011.
- Evaristo, R., Bals-Elsholz, T., Williams, E., Smalley, D., Donovan, M. and Fenn, A., "Relationship of graupel shape to differential reflectivity: theory and observations", *29th Conf. on Environ. Info. Processing Tech.*, Austin, TX, 5-10 January, 2013.
- Hudak, D., Currie, B., Rodriguez, P., Cober, S., Zawadzki, I., Isaac, G. and Wolde, M., "Cloud phase detection in winter stratiform clouds using Polarimetric Doppler Radar", *Proceedings of ERAD*, pp. 90-94, 2002.
- Ikeda, K., Rasmussen, R., Brandes, E. and McDonough, F., "Freezing Drizzle Detection with WSR-88D Radars", *J. Appl. Meteor. Climatol.*, **48**, 41–60, 2009. [doi: 10.1175/2008JAMC1939.1]
- Johnston, C., Serke, D., Adriaansen, D., Reehorst, A., Politovich, M., Wolff, C. and McDonough, F., "Comparison of in-situ, model and ground based in-flight icing severity", *AMS Conference Preprint*, Seattle, WA, Jan 24-27, 2011.
- Plummer, D., Göke, S., Rauber, R. and Di Girolamo, L., "Discrimination of mixed- versus ice-phase clouds using dual-polarization radar with application to detection of aircraft icing regions", *J. of Appl. Meteor. and Clim.*, **49**, Issue 5, pp. 920-936, 2010. [doi: 10.1175/2009JAMC2267.1]
- Politovich, M.K., B.B. Stankov and B.E. Martner, "Determination of liquid water altitudes using combined remote sensors", *J. Appl. Meteor.*, **34**, pp. 2060—2075, 1995.
- Reehorst, A., L.; Brinker, D., J.; and Ratvasky, T., P., "NASA Icing Remote Sensing System Comparisons from AIRS II". *NASA/TM--2005-213592 (AIAA-2005-0253)*, 2005.
- Reehorst, A., Politovich, M., Zednik, S., Isaac, G. and Cober, S., "Progress in the development of practical remote detection of icing conditions", *NASA/TM 2006-214242*, NASA, 2006.

Serke, D., J., Hubbert, S. Ellis, A. Reehorst, P. Kennedy, D. Albo, A. Weekley and M. Politovich, 2011: "The winter 2010 FRONT/NIRSS in-flight icing detection field campaign", *AMS 35th Conf. on Radar Meteor.*, Pittsburgh, PA, 26-30 September, Available online.

Serke, D., Ellis, S., Reehorst, A., Hubbert, J., Albo, D., Weekley, A., Adriaansen, D., Gaydos, A. and Politovich, M., "Progress toward a volumetric in-flight icing hazard system for airports which incorporates operational dual-polarization S-band radars", *7th European Conf. on Radar in Meteor. and Hydro.*, June 24-29, Toulouse, FR, 2012.

Smalley, D., Bennett, B., Hallowell, R., Donovan, M., and Williams, E., "Development of dual polarization aviation weather products for the FAA", *AMS Conference Preprint*, 2009.

Solheim, F., Godwin, J., Westwater, E., Han, Y., Keihm, S., Marsh, K., and Ware, R., "Radiometric profiling of temperature, water vapor and cloud liquid water using various inversion methods", *Radio Sci.*, **33**, pp. 393-404, 1998.